

INTRODUCTION: 62295 is a mesostasis-rich, basaltic impact melt that is unique in being very magnesian and rich in olivine and spinel. Macroscopically it is greenish-gray in color and quite tough (Fig. 1). It was collected ~35 m southwest of Buster Crater. Zap pits are abundant on the “lunar top” surface, rare to absent on other surfaces.



FIGURE 1. S-72-38399.

PETROLOGY: General petrographic descriptions are given by Agrell et al. (1973), Brown et al. (1973), Hodges and Kushiro (1973), Walker et al. (1973), Nord et al. (1973), Weiblen and Roedder (1973), McGee et al. (1979) and Vaniman and Papike (1981). Steele and Smith (1975) provide data on minor elements in olivines. Nord et al. (1973) studied mineral structures using high-voltage transmission electron spectroscopy (HVTEM). Misra and Taylor (1975) report metal compositions. Melt inclusions were studied by Weiblen and Roedder (1973).

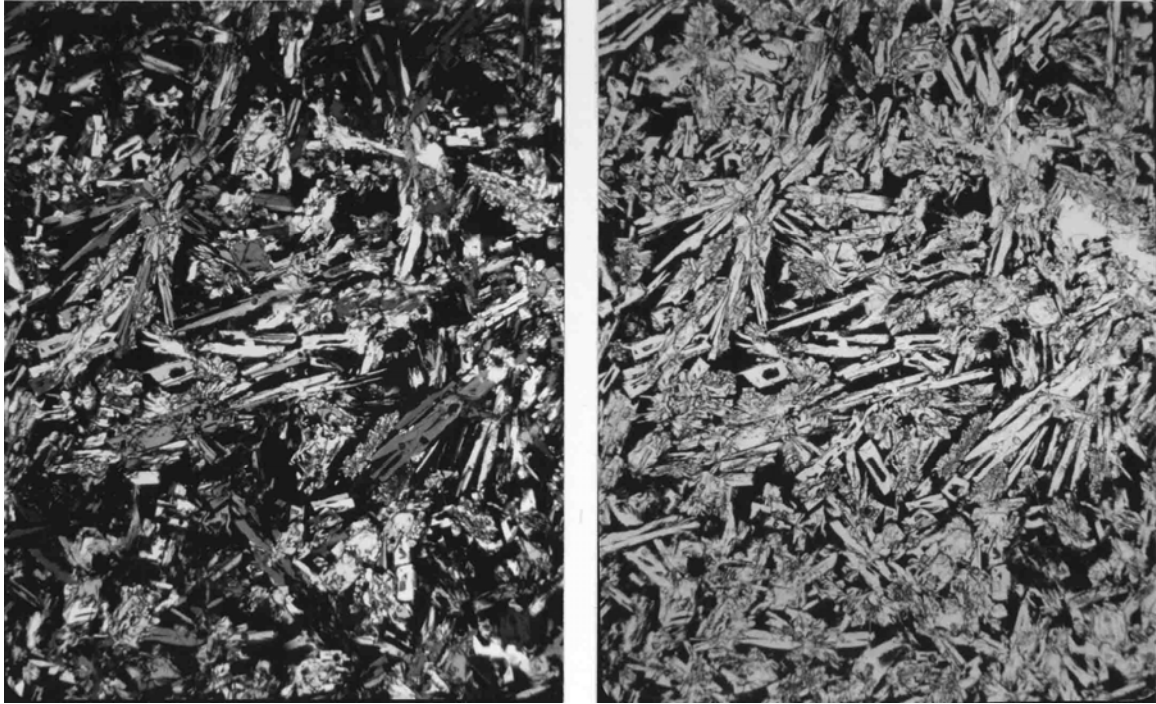


FIGURE 2. 62295,69, general view. Width 2 mm.
a) xpl. b) ppl.

62295 is a fine-grained, mesostasis-rich basaltic impact melt with the mineralogy of a spinel troctolite (Fig. 2). It is somewhat heterogeneous on the thin section scale, an approximate mode being 55% plagioclase, 25% olivine, 15% mesostasis and 5% spinel. Xenocrysts (up to 1.5 mm) of olivine (Fo₉₀₋₉₅), plagioclase (An₉₄₋₉₉), pink spinel (9-16 mol% chromite) and metal are preserved in a finer-grained matrix (<1 mm) characterized by a variety of quench textures. Normally-zoned olivine (Fo₇₈₋₉₂) and plagioclase (An₉₀₋₉₆) are the principal matrix minerals and occur as hollow, euhedral laths and skeletal grains, as variolitic to graphic intergrowths and as clots with a feathery to spinifex texture. Inclusions of a colorless to pale yellow spinel (2-4 mol% chromite) are abundant in both matrix olivine and plagioclase. These spinels are metastable and their existence implies rapid cooling and crystal growth rates. A complex, cryptocrystalline mesostasis of plagioclase, olivine, clinopyroxene, metal, troilite, schreibersite and a fluor-phosphate fills interstices and hollow crystals. The pyroxenes are ferroaugites (Fig. 3) and occur only in the mesostasis. Metal shows a large range in composition (Fig. 4). Co-existing schreibersite is unusually rich in Ni (~42% Ni) (see Misra and Taylor, 1975; Brown et al., 1973; Weiblen and Roedder, 1973 for other metal data).

The xenocrysts are inhomogeneously distributed through the rock and often core the radiate intergrowths mentioned above; all are mantled by fine-grained reaction rims. Several authors note that the xenocryst population is mineralogically similar to the pink spinel troctolite (PST) clast in 67435. Steele and Smith (1975) find the xenocryst olivines to be poor in minor elements (except Cr) compared to matrix olivines (Table 1).

Roedder and Weiblen (1977b) describe an unusual chondrule-like particle consisting of a single crystal of barred olivine with thin stringers of plagioclase and opaques separating the bars. The olivine shows reverse zoning with an intermediate area more magnesian (Fo_{92}) than either the core or rim (both Fo_{88}). The plagioclase stringers bear no crystallographic relation to the olivine and thus are not exsolution lamellae.

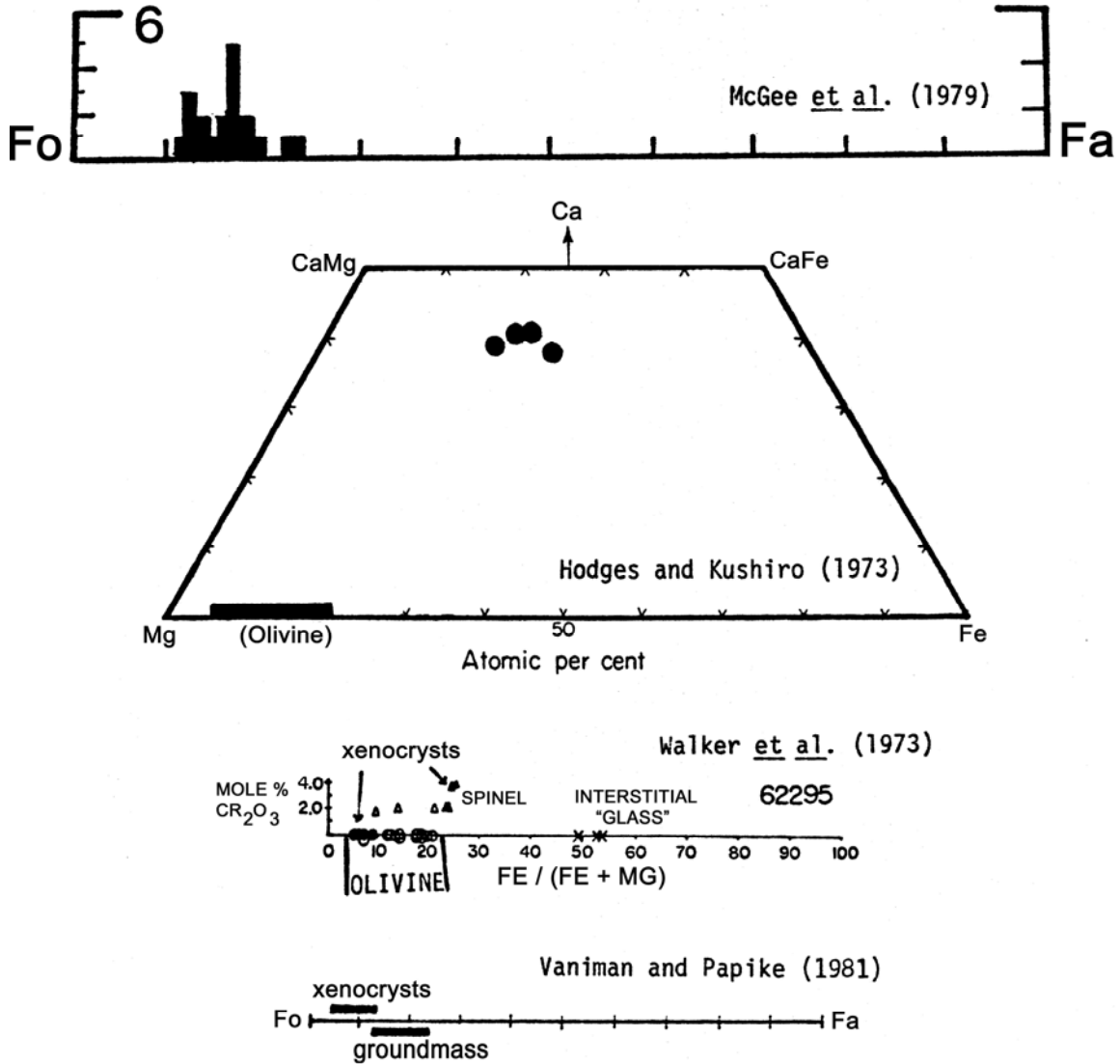


FIGURE 3a. Mafic mineral compositions.

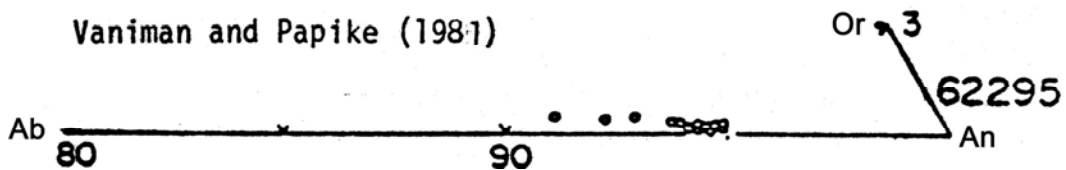
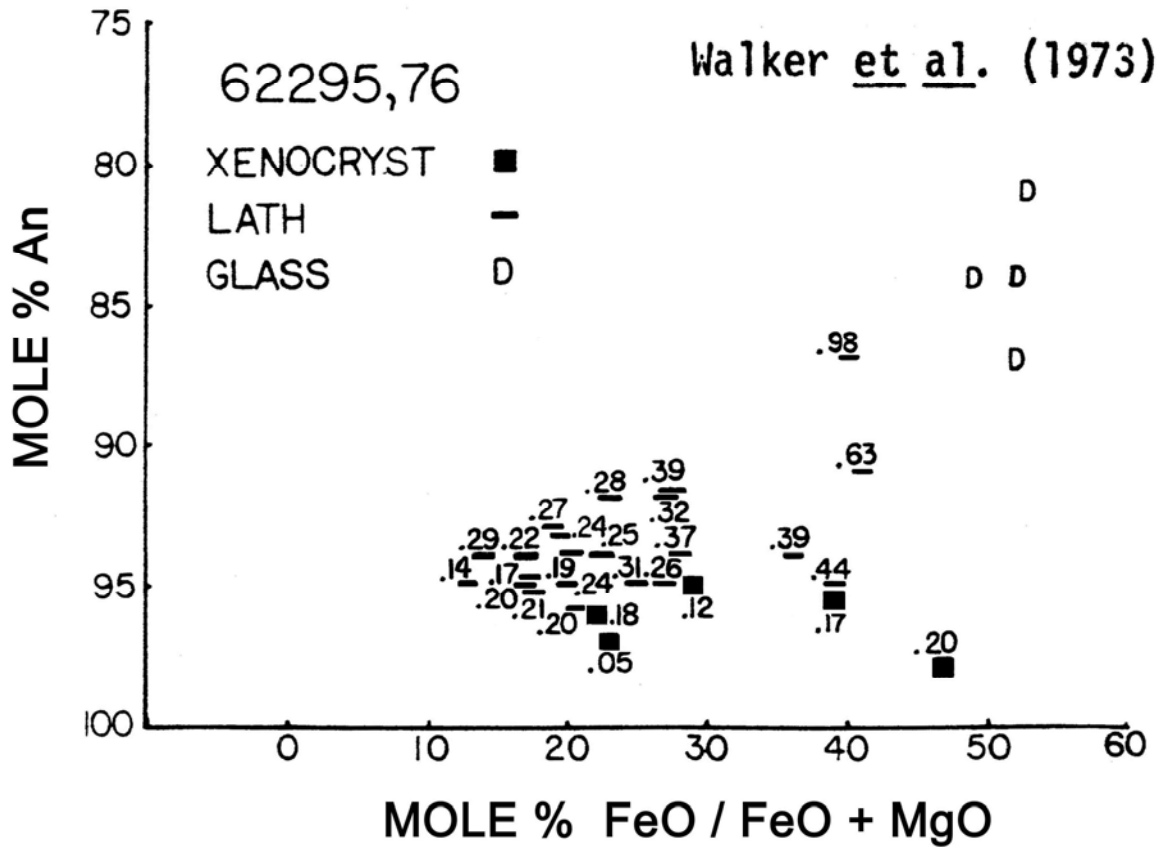
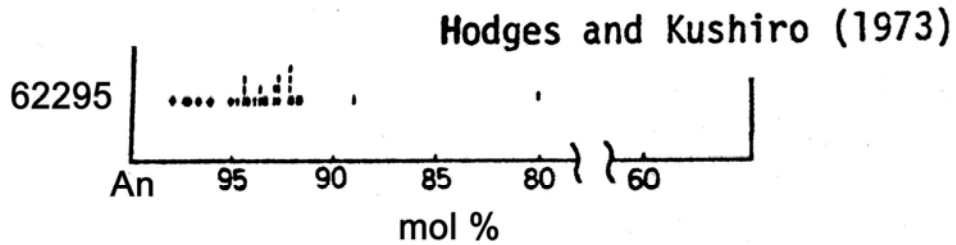
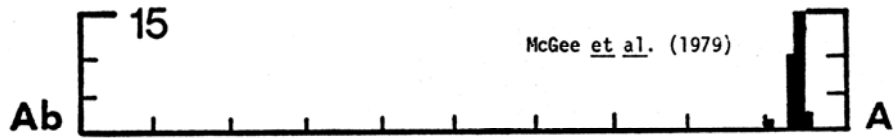


FIGURE 3b. Plagioclase compositions.

EXPERIMENTAL PETROLOGY: Crystallization experiments on the 62295 composition are reported by Walker et al. (1973), Hodges and Kushiro (1973) and Ford et al. (1974). All authors find spinel to be the liquidus phase at all pressures. At low pressure spinel is followed by olivine, plagioclase and pyroxene with decreasing temperature. Below ~1250°C and at low pressure, spinel reacts with the liquid to form olivine, and plagioclase. At progressively higher pressures the spinel field expands and olivine is replaced by pyroxene. There is no approach to multiply saturated conditions with increasing pressure (Figs. 5, 6).

This crystallization sequence (spinel, olivine, plagioclase, pyroxene) is consistent with that predicted by low pressure phase diagrams (Fig. 7) and determined by textural studies (e.g. Engelhardt, 1978). Data from silicate melt inclusions (Weiblen and Roedder, 1973) are in basic agreement with this sequence except for apparently requiring a minor amount of a Ti-rich phase to follow olivine and precede plagioclase (Fig. 8).

L.A. Taylor et al. (1976) performed subsolidus heating experiments on natural rock chips to observe changes in metal composition and morphology. Their results are summarized in Figure 9.

TABLE 1. Minor elements in 62295 olivine (Steele and Smith, 1975).

	CaO	TiO ₂	MnO	Al ₂ O ₃	Cr ₂ O ₃
Matrix	0.250	0.017	0.092	0.130	0.087
Xenocryst	0.060	0.009	0.045	0.048	0.124

Oxides in wt%

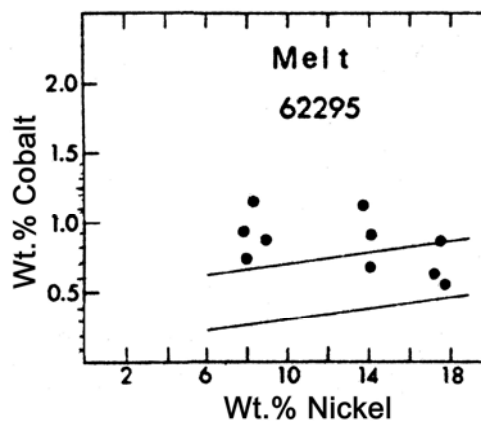


FIGURE 4. Metals; from Misra and Taylor (1975).

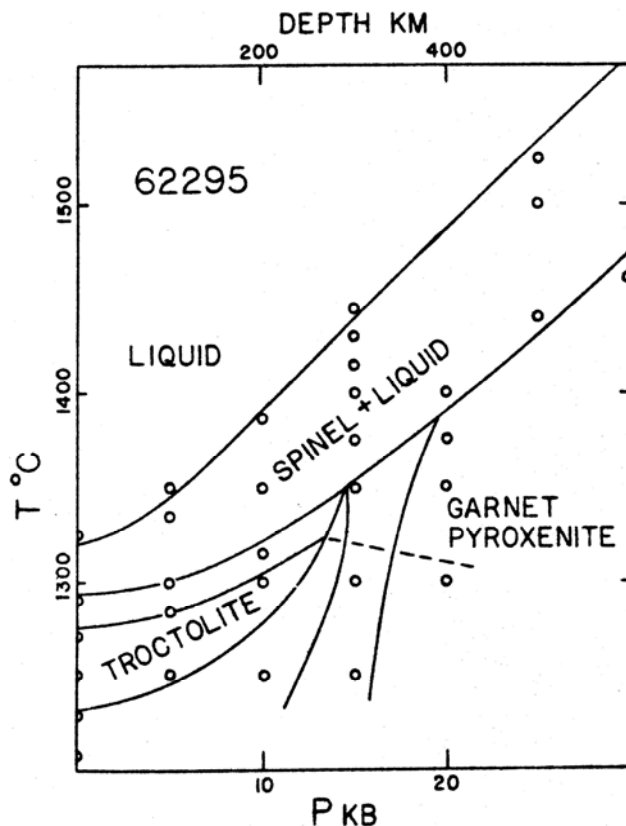


FIGURE 5. From Walker et al. (1973).

CHEMISTRY: Major and trace element analyses are provided by Hubbard et al. (1973), Rose et al. (1973) and Wanke et al. (1976). Krahenbuhl et al. (1973) give siderophile and volatile element data and Eldridge et al. (1973) report natural and cosmogenic radionuclide abundances. Walker et al. (1973) present major elements obtained by electron microprobe analyses of natural rock powder fused to a glass. Other chemical data are found in the work of geochronologists (referenced below).

62295 is among the most magnesian, and has one of the highest Mg/Fe (Mg/Mg+Fe molar = 0.81), of any lunar impact melt analyzed (Table 2). Nonetheless it is chemically distinct from the ultramafic PST clast in 67435 which contains ~34% MgO. Lithophile elements (Fig. 10) are slightly enriched over local soils and are dominated by KREEP. Eldridge et al. (1973) note the low K/U ratio (770); Th/U is typical of lunar rocks (3.9). The siderophile elements indicate a meteoritic component (Table 2). Ganapathy et al. (1973) mention the high Ge content (642 ppb) but do not consider it inactive of fumarolic volatiles due to the normal volatile to involatile ratios (e.g. Tl/Cs and Tl/U) of the rock. Hertogen et al. (1977) assign this sample to meteoritic group IH, a group largely restricted to Apollo 16.

STABLE ISOTOPES: Taylor and Epstein (1973) report whole rock δO^{18} and δSi^{30} values of +5.81 and -0.27 ‰ respectively.

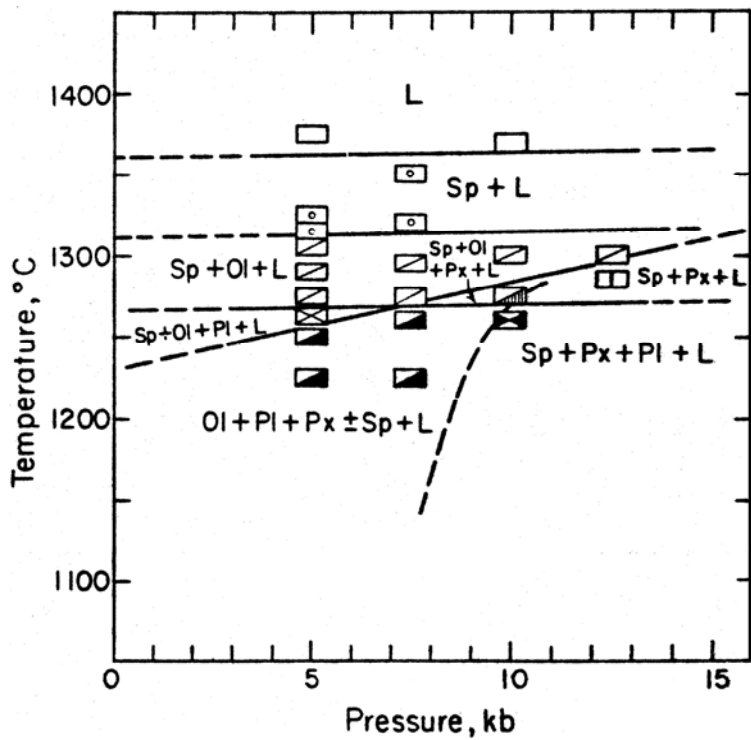


FIGURE 6. From Hodges and Kushiro (1973).

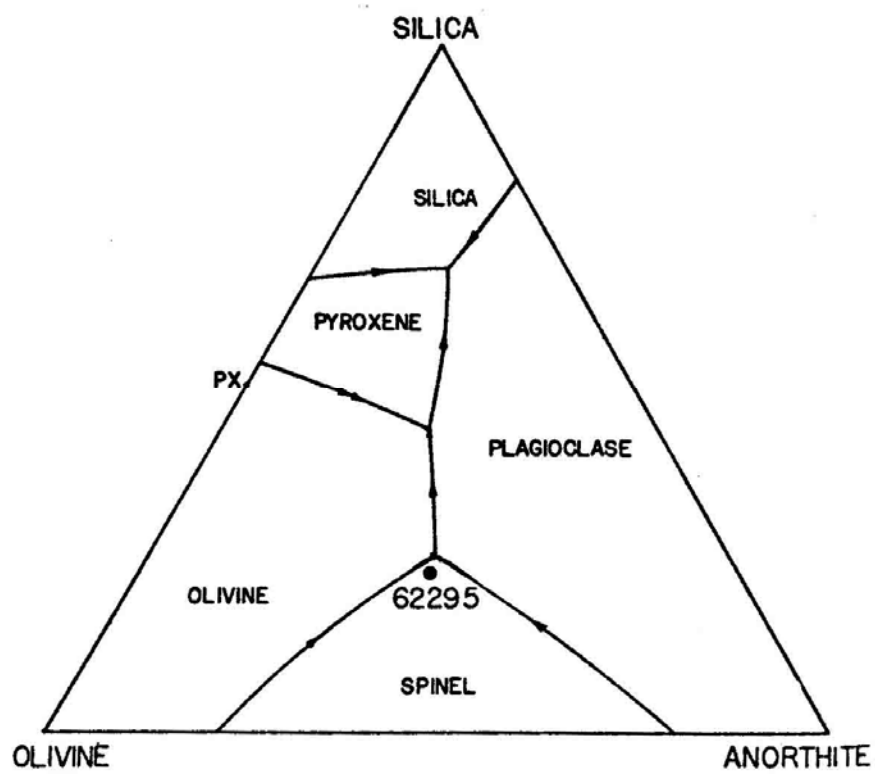


FIGURE 7. From Walker et al. (1973).

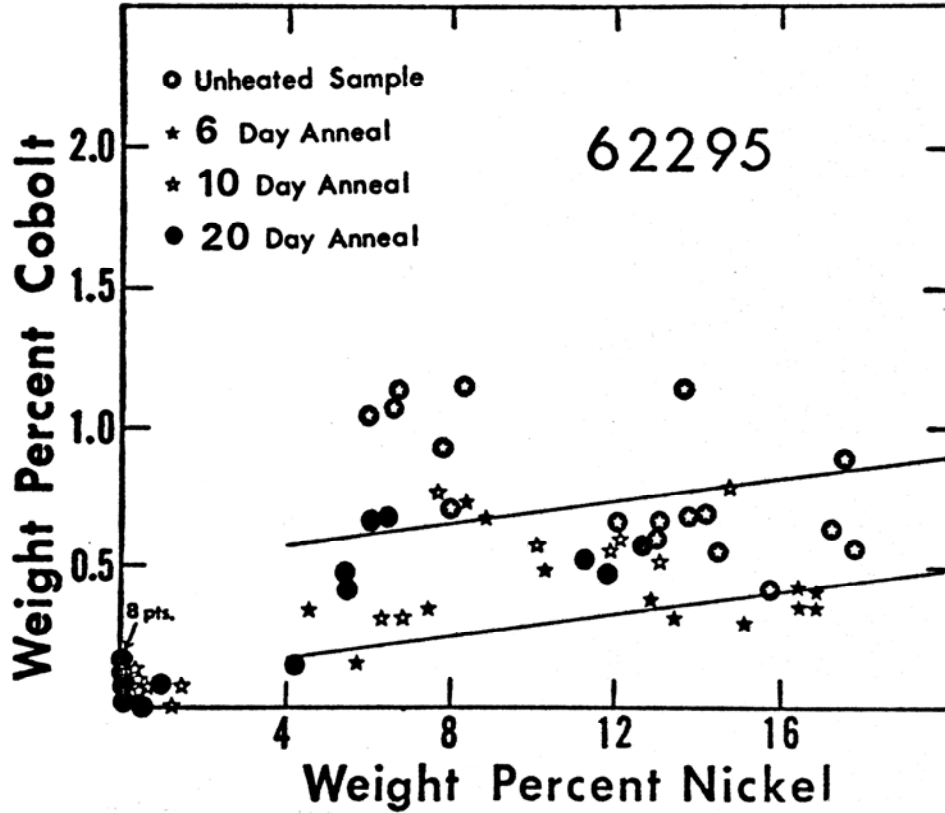


FIGURE 9. From L.A. Taylor et al. (1976).

TABLE 2. Summary chemistry of 62295.

SiO ₂	45.3	Sr	131
TiO ₂	0.72	La	19
Al ₂ O ₃	20.5	Lu	0.88
Cr ₂ O ₃	0.17	Rb	5.2
FeO	6.2	Sc	10
MnO	0.09	Ni	285
MgO	14.7	Co	25
CaO	11.6	Ir ppb	4.3
Na ₂ O	0.45	Au ppb	5.1
K ₂ O	0.08	C	
P ₂ O ₅	0.14	N	
		S	700
		Zn	18.9
		Cu	14.1

Oxides in wt%, others in ppm
 except as noted.

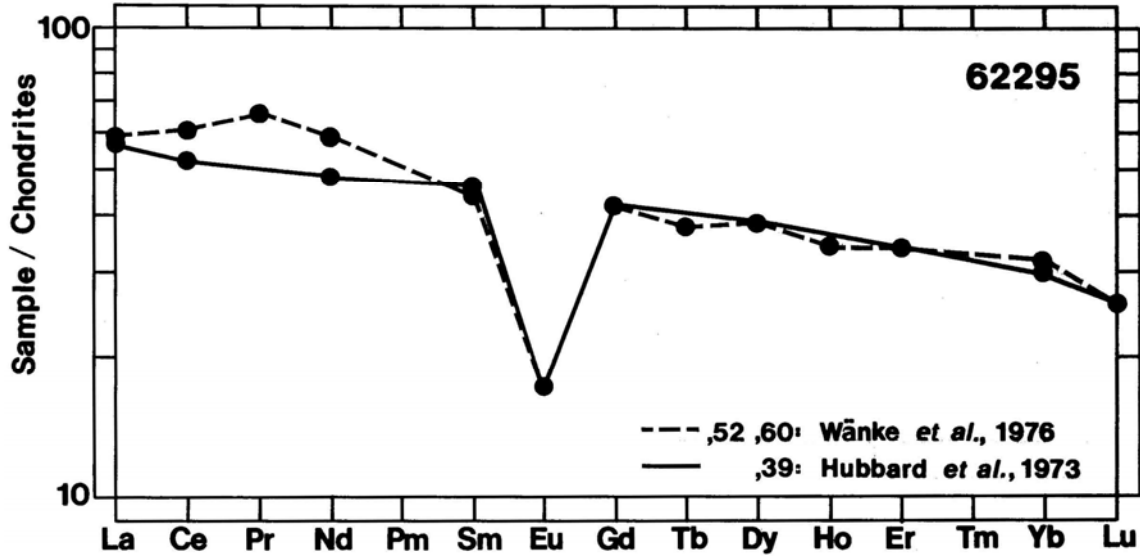


FIGURE 10. Rare earth elements.

TABLE 3. Summary of whole rock Rb-Sr data for 62295.

	$\frac{^{87}\text{Rb}}{^{86}\text{Rb}}$	$\frac{^{87}\text{Sr}/^{86}\text{Sr}}$ measured	$\frac{^{87}\text{Sr}/^{86}\text{Sr}}$ at 4.6 b.y.*	T_{BABI} (b.y.)	T_{LUNI} (b.y.)	Reference
62295,34	0.0958	0.70501	0.69955	4.31	4.38	Nyquist <i>et al.</i> (1973)
,34 II	0.0994	0.70519	0.69946	4.28	4.35	Nyquist <i>et al.</i> (1973)
,35	0.0877	0.70452	0.69956	4.39	4.46	Mark <i>et al.</i> (1974)

*corrected for interlaboratory bias by Nyquist (1977)

Turner et al. (1973) could not obtain a good ^{39}Ar - ^{40}Ar plateau due to equipment problems during the low temperature release, but an age of 3.89 ± 0.05 b.y. was inferred from the 900° and 1000° release data. A maximum age of 3.91 ± 0.05 b.y. was also calculated (Fig. 12). The total Ar release age is 3.31 b.y.

RARE GAS/EXPOSURE HISTORY: From fossil track analyses Bhandari et al. (1973) infer that 62295 had a simple exposure history without shallow burial exposure in the regolith. A surface exposure age of 2.7 m.y. was calculated. Turner et al. (1973) report cosmogenic Ar isotope ratios and calculate an Ar exposure age of 310 m.y. Marti (1974, pers. comm., referenced in Horz et al., 1975) determined a Kr exposure age of 235 m.y. Eldridge et al. (1973) provide short-lived cosmogenic radionuclide abundances and Lightner and Marti (1974b) report various Xe isotope concentrations.

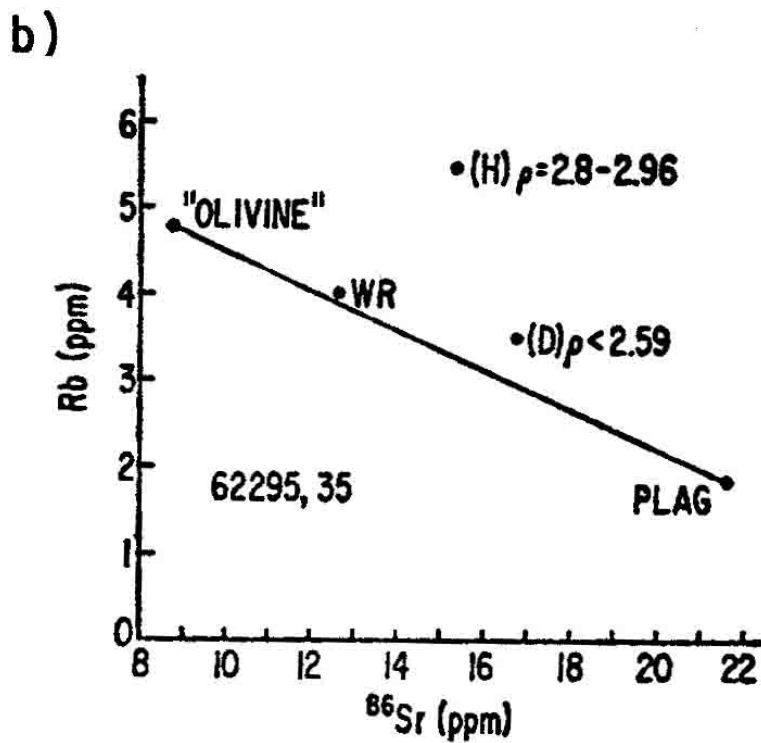
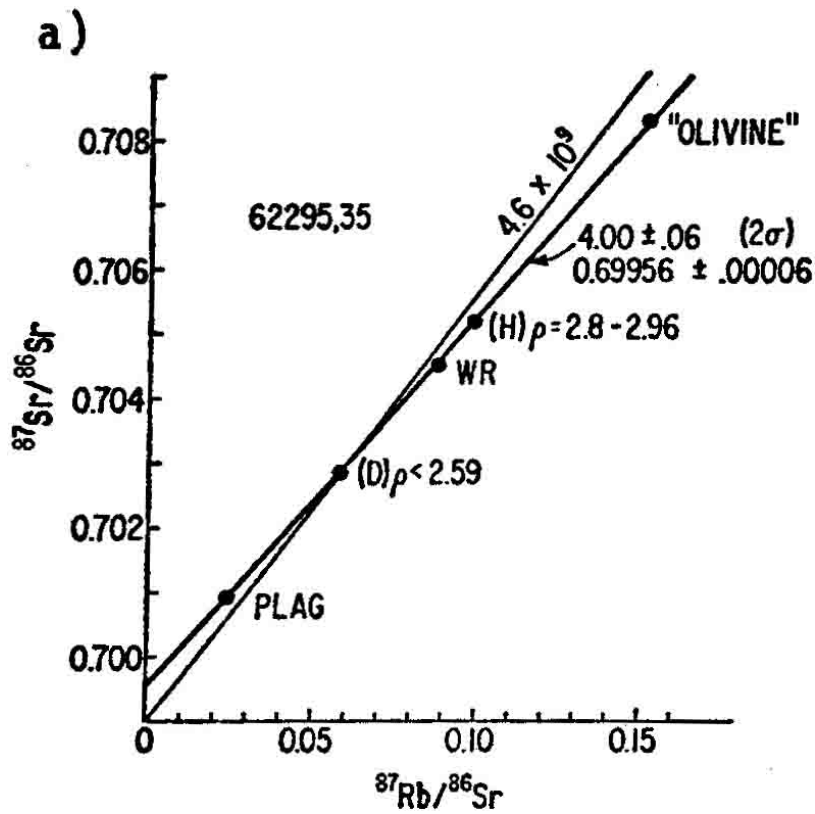


FIGURE 11. Rb-Sr data.
 a) isochron. b) Rb v. ^{86}Sr ; from Mark et al. (1974).

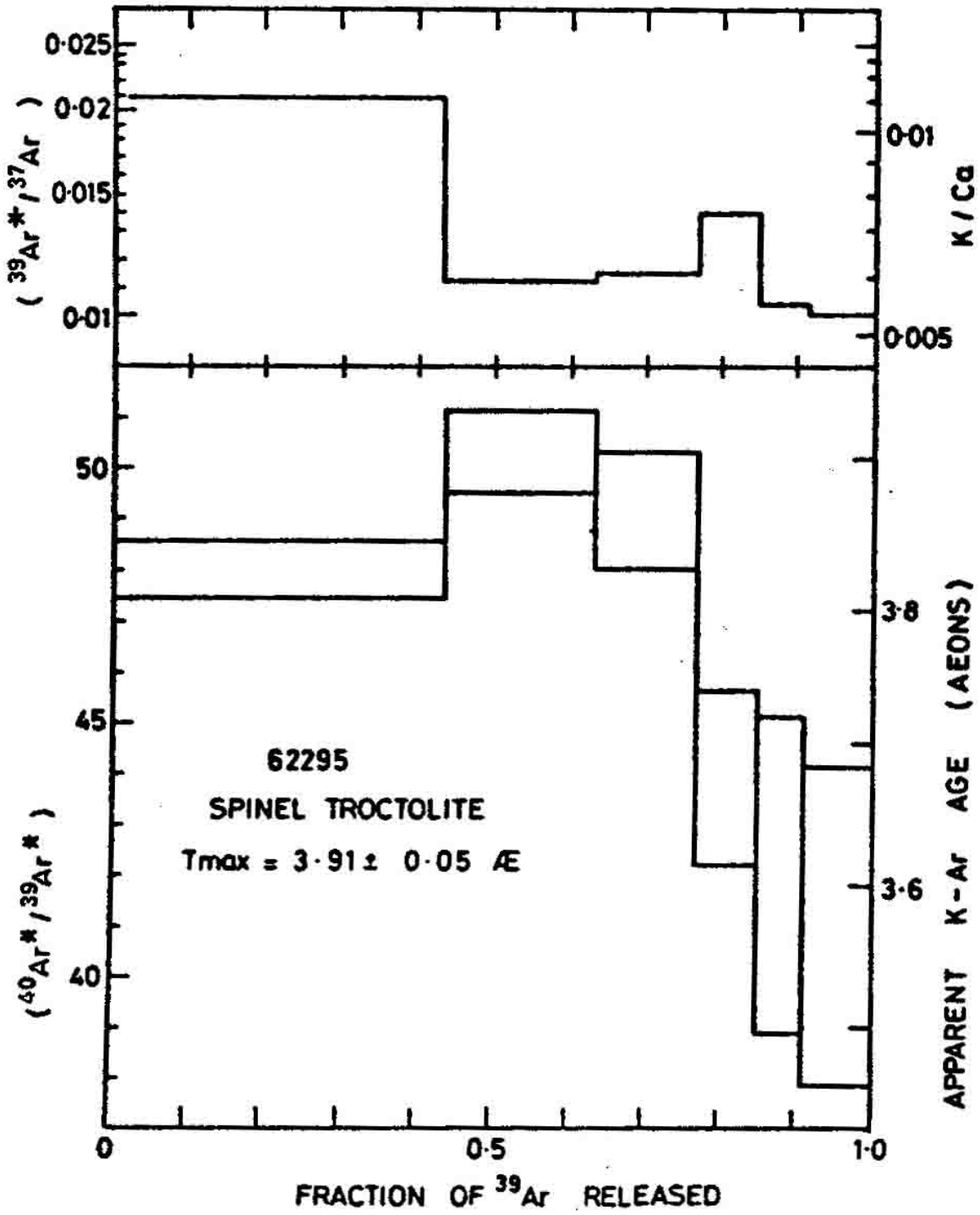


FIGURE 12. Ar release; from Turner et al. (1973).

MICROCRATERS: Morrison et al. (1973) and Neukum et al. (1973) provide size-frequency data. Microcraters occur on only one surface indicating a simple exposure history. The cratered surface is probably still in production.

PHYSICAL PROPERTIES: Magnetic and mossbauer studies by Brecher et al. (1973) indicate that 62295 contains 0.37 wt% metal, predominantly as coarse, multidomain particles. There is also a small but significant fraction of single domain grains which are capable of carrying a relatively stable component of natural remanence (Figs. 13, 14). Remanent properties of different chips scatter over an order of magnitude due to the inhomogeneous distribution of metal and the ability of the chips to acquire a viscous remanence. Cyclical heating experiments produced irreversible changes in the magnetic properties through the subsolidus reduction of Fe^{2+} to produce new metal grains and the coalescence of preexisting metal grains.

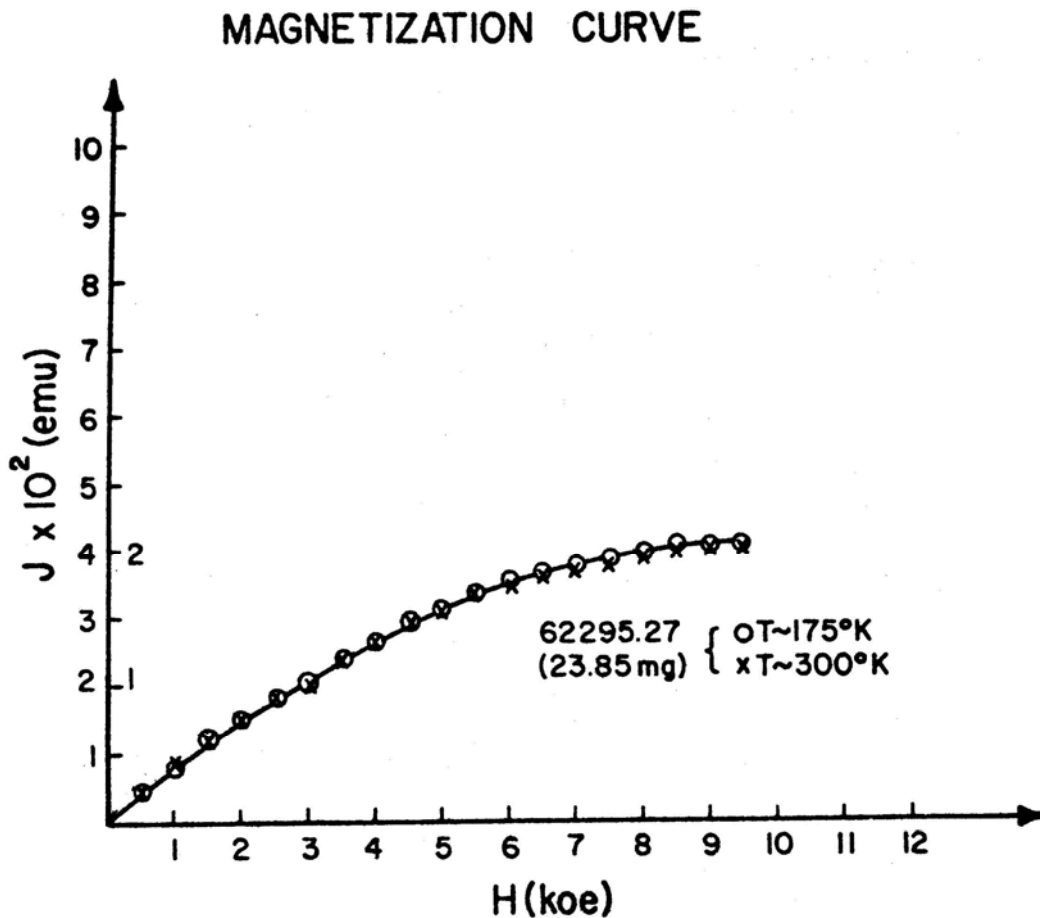


FIGURE 13. Magnetic behavior; from Brecher et al. (1973).

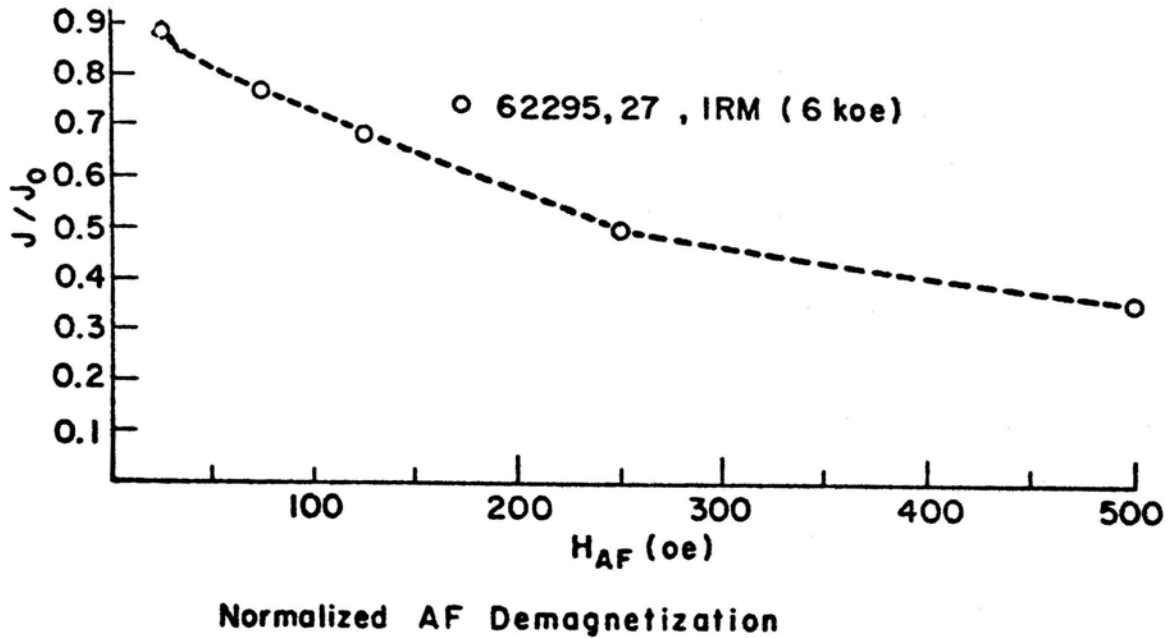


FIGURE 14. IRM stability; from Brecher et al. (1973).

Todd et al. (1973) and Wang et al. (1973) report elastic property measurements under confining pressures of 1-5000 bars (Fig. 15). Todd et al. (1973) also calculate and measure values of the mean volume thermal expansion coefficient over the range 25-200%. The calculated value ($16.9^{\circ}\text{C}^{-1}$) was an order of magnitude greater than the measured value (6.8°C^{-1}) apparently due to the presence of void space in the rock into which the minerals were able to expand.

Katsube and Collett (1973a,b) present and discuss measurements of the electrical characteristics of the rock (Fig. 16).

PROCESSING AND SUBDIVISIONS: In 1972, 62295 was broken along a natural fracture into three main pieces (.4, .5 and .6). That same year, .5 was sawn into many pieces (Fig. 17) and widely allocated. .6 was cut into two pieces and then broken up into smaller chips for allocation and storage. In 1975, .4 was sawn into two pieces (.4 and .122) and the smaller of these (.122) sent to the Brooks remote storage vault. Most of the thin sections were made from .12 (a portion of .5) and .45 (a portion of .6). .46 (a 5.41 g split of .6) was homogenized to a 100 mesh powder for 0.5 g allocations to the experimental petrologists. 2.17 g of this powder remains. The largest single pieces remaining today are .4 (108.5 g) at JSC and .122 (48.1 g) at Brooks.

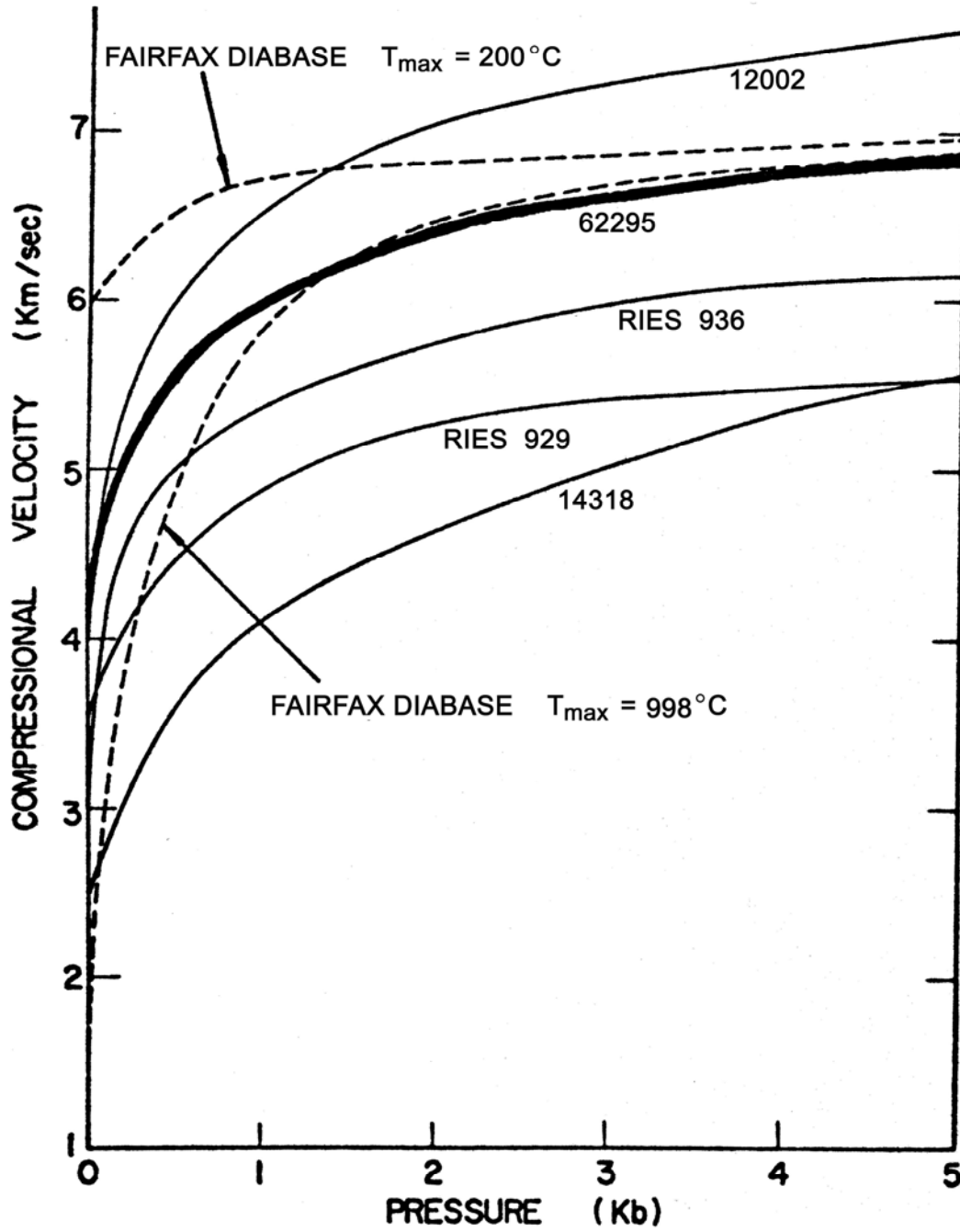


FIGURE 15. Elastic properties; from Todd et al. (1973).

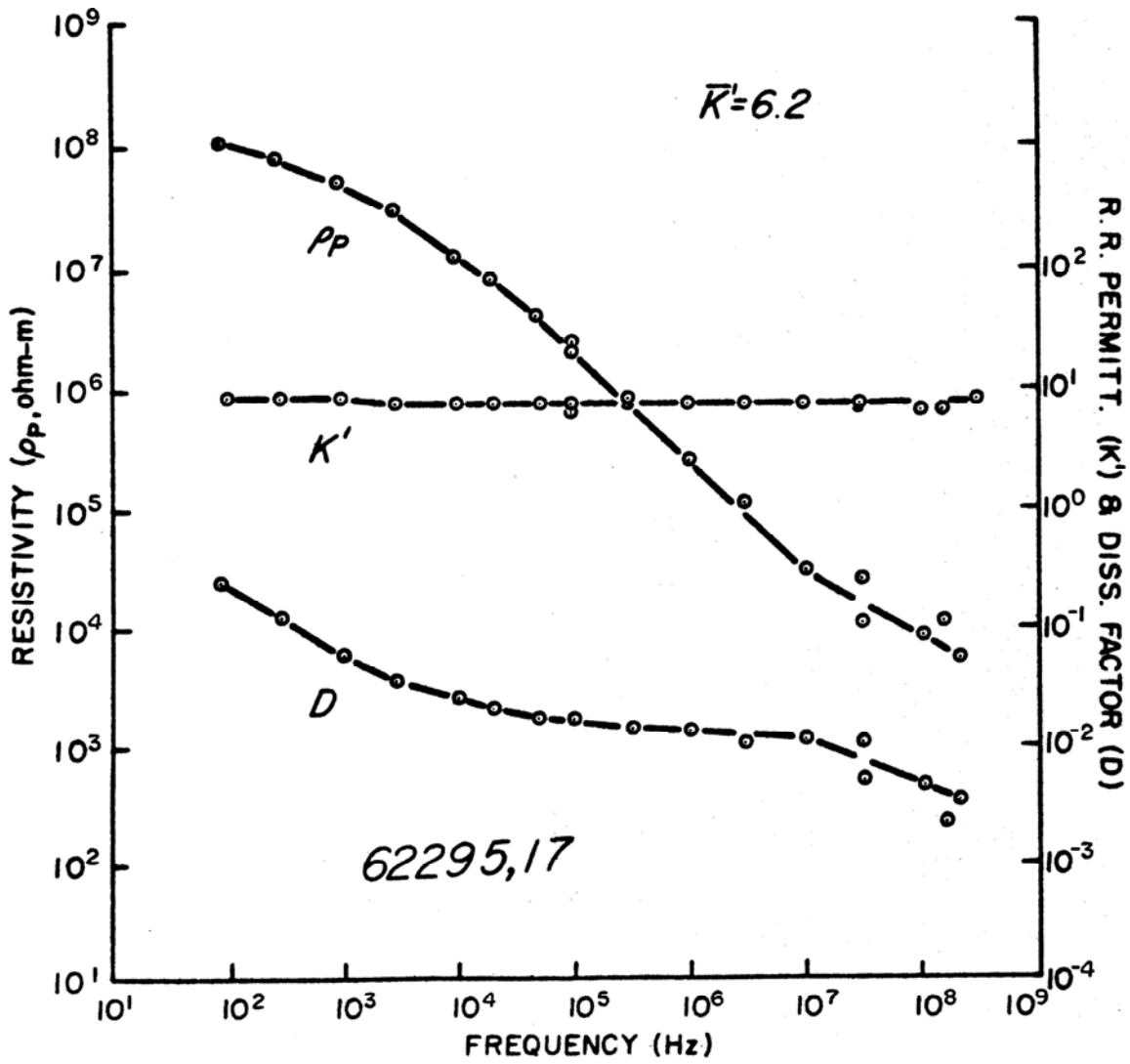


FIGURE 16. Electrical characteristics;
from Katsube and Collett (1973a, b).

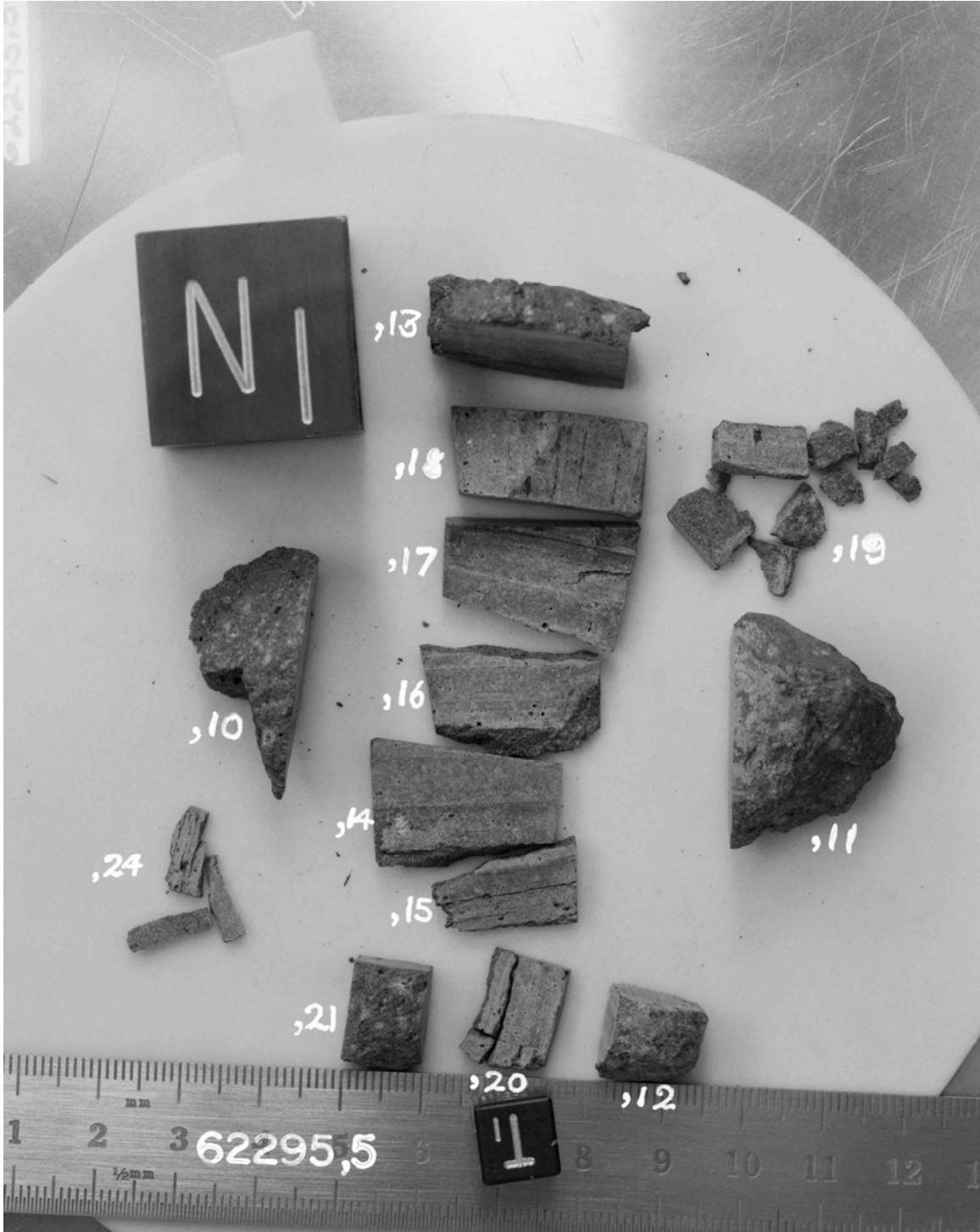


FIGURE 17. Subdivisions following sawing. S-72-50655.